Available online at www.sciencedirect.com
SCIENCE DIRECT®
ELSEVIER
Nuclear Physics A 720 (2003) 20–42
NUCLEAR PHYSICS A
www.elsevier.com/locate/npe

$^3P_2$–$^3F_2$ pairing in dense neutron matter: the spectrum of solutions

M.V. Zverev [a], J.W. Clark [b,*], V.A. Khodel [a,b]

[a] *Russian Research Center Kurchatov Institute, Moscow 123182, Russia*
[b] *McDonnell Center for the Space Sciences and Department of Physics, Washington University, St. Louis, MO 63130-4899, USA*

Received 24 December 2002; accepted 21 January 2003

Abstract

The $^3P_2$–$^3F_2$ pairing model is generally considered to provide an adequate description of the superfluid states of neutron matter at densities some 2–3 times that of saturated symmetrical nuclear matter. The problem of solving the system of BCS gap equations expressing the $^3P_2$–$^3F_2$ model is attacked with the aid of the separation approach. This method, developed originally for quantitative study of *S*-wave pairing in the presence of strong short-range repulsions, serves effectively to reduce the coupled, singular, nonlinear BCS integral equations to a set of coupled algebraic equations. For the first time, sufficient precision becomes accessible to resolve small energy splittings between the different pairing states. Adopting a perturbative strategy, we are able to identify and characterize the full repertoire of real solutions of the $^3P_2$–$^3F_2$ pairing model, in the limiting regime of small tensor-coupling strength. The P–F channel coupling is seen to lift the striking parametric degeneracies revealed by a earlier separation treatment of the pure, uncoupled $^3P_2$ pairing problem. Remarkably, incisive and robust results are obtained solely on the basis of analytic arguments. Unlike the traditional Ginzburg–Landau approach, the analysis is not restricted to the immediate vicinity of the critical temperature, but is equally reliable at zero temperature. Interesting connections and contrasts are drawn between triplet pairing in dense neutron matter and triplet pairing in liquid ^{3}He.

PACS: 26.60.+c

* Corresponding author.
E-mail address: jwc@wuphys.wustl.edu (J.W. Clark).

0375-9474/03/$ – see front matter
doi:10.1016/S0375-9474(03)00653-5

1. Introduction

It is widely accepted that triplet pairing between constituent spin-1/2 fermions gives rise to superfluid phases in liquid ^{3}He at milli-Kelvin temperatures and in the neutronic component of the quantum fluid interior of a neutron star at temperatures in the hundred keV range and below. In both cases, the density is so high that the familiar singlet S-wave gap is quenched by the dominant effect of the short-range repulsion in that channel. Instead, pairing is favored in a channel with an odd orbital momentum $L = 1$, and therefore in the triplet spin state. The pairing mechanisms active in these two examples produce interesting distinctions between them. In superfluid ^{3}He, pairing is triggered by spin fluctuations [1], and the B-state (or B-phase) with total angular momentum $J = 0$ occupies most of the superfluid phase diagram. However, the spin-fluctuation mechanism induces relatively tiny energy splittings between states with different J values. Consequently, very close to the critical temperature T_c there exists a phase transition from the B-phase to the A-phase, which involves a combination of $J = 1$ and $J = 2$ pairing channels.

The situation in neutron matter is rather different. Referring to the experimental data on the energy dependence of the *nn* scattering phase shifts [2], one may infer that central forces between a neutron pair are quite weak, and that pairing must be due predominantly to the spin–orbit force. Based on empirical analyses of spin–orbit splitting in finite nuclei, the latter force is expected to be insensitive to polarization and correlation effects. The spin–orbit pairing mechanism implies that the spin $\mathbf{S}$ and orbital momentum $\mathbf{L}$ of the pair cease to be conserved separately, and pairing in the $J = 2$ channel dominates [3–9].

In both Fermi quantum liquids, the effective in-medium interaction contains a component that mixes two-body states with orbital angular momenta $L \pm 2$. Specifically, pairing channels with $L = 1$ and $L = 3$ are coupled by the magnetic dipole force in the case of liquid ^{3}He and by the tensor force arising from pion exchange, in neutron matter. However, the effect is of minuscule importance in the ^{3}He problem, since the magnetic dipole component is smaller in magnitude than the dominant central part of the interaction by a factor 10^{-7} [1]. By contrast, the magnitude of the dominant spin–orbit force in neutron matter is only a few times larger than the tensor component, so the effects of the latter cannot be neglected. (More specifically, the parameter measuring the strength of the tensor force relative to the spin–orbit force varies around 0.3 in the density interval $\rho_0 < \rho < 3\rho_0$ [9,10] if in-vacuum interaction constants are adopted, ρ_0 being the saturation density of symmetrical nuclear matter.) Moreover, pion exchange is responsible for the most powerful fluctuations in neutron matter. Accordingly, it is imperative to give careful attention to $^3\mathrm{P}_2$–$^3\mathrm{F}_2$ channel coupling in the quantitative description of pairing in neutron matter.

Reliable prediction of the phase diagram of triplet pairing over an extensive temperature range has proven to be extraordinarily difficult. The traditional tool for elucidation of the phase diagram in liquid ^{3}He and other systems manifesting superfluidity or superconductivity has been the Ginzburg–Landau functional approach. But since Ginzburg–Landau theory is valid only near the critical temperature, it has little relevance to neutron stars, which cool down to temperatures one or two orders of magnitude below T_c by a thousand years after their birth in a supernova event. There is of course the alternative of brute-force iterative solution of the gap equation, which has been widely used in quantitative studies of singlet S-wave pairing [11]. However, this strategy is generally afflicted with slow conver-

gence and uncertain accuracy both for S-wave interactions containing strong short-range repulsions and for pairing in higher angular momentum states, where one must deal with a multitude of coupled nonlinear singular integral equations. The limitations of standard iterative approaches become particularly serious when one seeks to construct the superfluid phase diagram of the system, which is sensitive to tiny energy splittings between the different solutions of the BCS pairing problem.

Explication of the complete superfluid phase diagram of neutron matter has two facets. First, one must identify and characterize the set of admissible solutions of the BCS gap equations arising in the $^3P_2$–$^3F_2$ pairing problem, i.e., one must find the "spectrum of solutions". Second, one must determine the relative stability of the different solutions under variation of density, temperature, and other relevant parameters, so as to uncover the possible phase transitions and map out the actual phase diagram.

The purpose of this paper is to present a detailed account of the substantial progress that has been made on the first of these tasks through application of the separation method developed in Refs. [8,12] for robust and accurate solution of BCS gap equations. (The reader may consult Ref. [13] for a comprehensive review of the separation approach.) Many of the results obtained here have been exposed in condensed form in earlier works [8,14]; it is our intent here to offer a more complete justification of these findings, and to provide an enhanced understanding of their wider implications.

In the separation method, the BCS system is recast so as to isolate the major, logarithmically divergent contributions to the pairing effect and treat them separately from the remaining features of the problem, which are very insensitive to the presence of the gap and its particular value. This method, which in essence reduces the problem to solution of system of algebraic equations, is equally reliable and precise in the limiting regimes $T \to T_c$ and $T \to 0$, as well as in between. In concrete calculations, we may accommodate and exploit the fact, based on the experimental P-scattering phases [2], that the central components of the in-vacuum *nn* interaction nearly compensate each other. We *assume*—quite plausibly—that this feature is maintained by the *effective nn* interaction within neutron matter. We furthermore assume—with less confidence—that the smallness of the parameter characterizing the importance of the tensor force relative to the spin–orbit force is maintained in dense neutron matter. It must be acknowledged that medium modification may be more significant in the case of the tensor force than it is for the spin–orbit component, especially in the vicinity of the phase transition leading to pion condensation [15,16]. Investigation of this issue calls for a concerted effort and will be pursued elsewhere.

The current study of the $^3P_2$–$^3F_2$ model is exhaustive in its assembly of the set of solutions whose structural expression involves only real numbers. The implementation of this program requires no numerical computations; remarkably, everything can be done analytically. In principle, the same method can be readily applied to the determination of complex solutions. However, this more complicated problem inevitably entails some computer work.

The paper is organized as follows: in Section 2, the coupled-channel BCS formalism is stated, the separation method is applied to the gap equations, and further analysis establishes the explicit equations of an incisive perturbative treatment of the $^3P_2$–$^3F_2$ pairing model. In Section 3, the parametric degeneracy inherent in the unperturbed $^3P_2$

problem is lifted, and all real solutions of the perturbed model are found. Section 4 furnishes a convenient and succinct catalog of these solutions. Finally, Section 5 is devoted to a discussion of potential vulnerabilities of our approach to the $^3P_2$–$^3F_2$ problem in neutron matter, as well as informative connections with aspects of triplet pairing in liquid ^{3}He.

2. The basic set of gap equations

Fixing the spin and isospin of the pairing state at $S = 1$ and $T = 1$ (triplet–triplet), we start with the partial-wave decomposition

$$\Delta_{\alpha\beta}(\mathbf{p}) = \sum_{J,L,M} \Delta_L^{JM}(p)\big(G_{LJ}^M(\mathbf{n})\big)_{\alpha\beta} \tag{1}$$

of the 2×2 gap matrix in terms of the spin-angle matrices

$$\big(G_{LJ}^M(\mathbf{n})\big)_{\alpha\beta} = \sum_{M_S M_L} C^{1M_S}_{\frac{1}{2}\frac{1}{2}\alpha\beta} C^{JM}_{1LM_S M_L} Y_{LM_L}(\mathbf{n}) \tag{2}$$

and the multichannel BCS gap equations

$$\begin{aligned}\Delta_L^{JM}(p) \;=\; & \sum_{L'L_1J_1M_1} (-1)^{1+\frac{L-L'}{2}} \iint \langle p|V^J_{LL'}|p_1\rangle S^{JMJ_1M_1}_{L'L_1}(\mathbf{n}_1) \\ & \times \frac{\tanh(E(\mathbf{p}_1)/2T)}{2E(\mathbf{p}_1)} \Delta_{L_1}^{J_1M_1}(p_1) p_1^2\, dp_1\, d\mathbf{n}_1,\end{aligned} \tag{3}$$

that embrace the formal problem to be solved [6–9]. The latter equations contain the spin trace

$$S^{JMJ_1M_1}_{LL_1}(\mathbf{n}) = \mathrm{Tr}\big[\big(G_L^{JM}(\mathbf{n})\big)^* G_{L_1}^{J_1M_1}(\mathbf{n})\big] \tag{4}$$

and the interaction matrix elements $\langle p|V^J_{LL'}|p_1\rangle$ appearing in the partial-wave expansion

$$V(\mathbf{p},\mathbf{p}_1) = \sum_{LL'JM} (-1)^{\frac{L-L'}{2}} \langle p|V^J_{LL'}|p_1\rangle G^M_{LJ}(\mathbf{n})\big(G^M_{L'J}(\mathbf{n}_1)\big)^*, \tag{5}$$

of the block of Feynman diagrams irreducible in the particle–particle channel. The quasiparticle energy

$$\begin{aligned}E(\mathbf{p}) \;&=\; \sqrt{\xi^2(p) + D^2(\mathbf{p})} \\ &=\; \left[\xi^2(p) + \frac{1}{2} \sum_{LJML_1J_1M_1} \big(\Delta_L^{JM}(p)\big)^* \Delta_{L_1}^{J_1M_1}(p) S^{JMJ_1M_1}_{LL_1}(\mathbf{n})\right]^{1/2}\end{aligned} \tag{6}$$

is assembled from the single-particle spectrum $\xi(p)$ of the normal Fermi liquid, measured relative to the chemical potential μ and often parametrized with an effective mass M^*, together with the gap components $\Delta_L^{JM}(p)$. We note that $E(\mathbf{p})$ takes on an angular dependence by virtue of the spin trace $S^{JMJ_1M_1}_{LL_1}(\mathbf{n})$, which in principle greatly complicates

the task of solving the system (3). However, this angular dependence only comes into play near the Fermi surface; hence it can be ignored in those integral contributions to the r.h.s. of Eq. (3) in which the region around the Fermi surface is suppressed [8,9]. Consequently, in practice the gap equations approximately decouple in the variables L', L_1, and J_1, by virtue of the orthogonality property

$$\int S_{LL_1}^{JMJ_1M_1}(\mathbf{n})\,d\mathbf{n} = \delta_{LL_1}\delta_{JJ_1}\delta_{MM_1}. \tag{7}$$

Treatment of the exact, coupled equations (3) is, therefore, not as difficult as it appears at first sight (though still not at all trivial).

The angle dependence of the function $D(\mathbf{p})$ makes it awkward to speak of *the* energy gap. Therefore, it is conventional to introduce the quantity

$$\Delta_{\mathrm{F}} = \left[\overline{D^2}(p_{\mathrm{F}})\right]^{1/2} \tag{8}$$

as a representative measure of the pairing gap in the quasiparticle spectrum, where the overbar signifies an angle average.

As we have argued in the introduction, the spin–orbit component of the neutron–neutron interaction exerts a strong influence on pair formation in dense neutron matter, favoring the condensation of pairs in the $^3\mathrm{P}_2$ state. Accepting this widely held view, the simplifying feature just revealed implies that contributions to triplet pairing from nondiagonal terms with $L', L_1 \neq 1$ or $J_1 \neq 2$ on the r.h.s. of Eq. (1) can be evaluated within perturbation theory. Defining $v_{\mathrm{F}} \equiv \langle p_{\mathrm{F}}|V_{11}^2|p_{\mathrm{F}}\rangle$, the relevant coupling parameter is $\eta = -\langle p_{\mathrm{F}}|V_{13}^2|p_{\mathrm{F}}\rangle/v_{\mathrm{F}}$. The evaluation is carried out in terms of the set of "principal" gap amplitudes $\Delta_1^{2M}(p)$, with M running from -2 to 2. A further simplification ensues from time-reversal invariance, which implies that only three of these five quantities can be independent, say $\Delta_1^{2M}(p)$ with $M = 0, 1, 2$.

Focusing on the nondiagonal contributions to the r.h.s. of Eq. (1), we observe that two of them are of leading significance. The first contains the integral of the product $V_{31}^2 S_{31}^{2M2M_1}\Delta_1^{2M_1}$, and the second contains the integral of the product $V_{11}^2 S_{13}^{2M2M_1}\Delta_3^{2M_1}$. Restricting attention to these contributions, we arrive at the $^3\mathrm{P}_2$–$^3\mathrm{F}_2$ pairing problem, which has been studied both analytically and numerically in earlier work [5,6,9,17]. The list of participating states appears to be exhausted upon addition of the $^3\mathrm{P}_0$ and $^3\mathrm{P}_1$ pairing channels, which are deemed to be of lesser importance; their role will be examined later in this paper.

Adopting the $^3\mathrm{P}_2$–$^3\mathrm{F}_2$ pairing model as circumscribed above, the BCS system (3) takes the explicit form

$$\begin{aligned}
&\Delta_1^{2M}(p) + \sum_{M_1}\int\!\!\int \langle p|V_{11}^2|p_1\rangle S_{11}^{2M2M_1}(\mathbf{n}_1)\frac{\tanh(E(\mathbf{p}_1)/2T)}{2E(\mathbf{p}_1)}\Delta_1^{2M_1}(p_1)p_1^2\,dp_1\,d\mathbf{n}_1 \\
&\quad = \sum_{M_1}\int\!\!\int \langle p|V_{13}^2|p_1\rangle S_{31}^{2M2M_1}(\mathbf{n}_1)\frac{\tanh(E_0(\mathbf{p}_1)/2T)}{2E_0(\mathbf{p}_1)}\Delta_1^{2M_1}(p_1)p_1^2\,dp_1\,d\mathbf{n}_1 \\
&\qquad + \sum_{M_1}\int\!\!\int \langle p|V_{11}^2|p_1\rangle S_{13}^{2M2M_1}(\mathbf{n}_1)\frac{\tanh(E_0(\mathbf{p}_1)/2T)}{2E_0(\mathbf{p}_1)}\Delta_3^{2M_1}(p_1)p_1^2\,dp_1\,d\mathbf{n}_1,
\end{aligned}$$

$$\Delta_3^{2M}(p) = \sum_{M_1} \int\int \langle p|V_{31}^2|p_1\rangle S_{11}^{2M2M_1}(\mathbf{n}_1) \frac{\tanh(E_0(\mathbf{p}_1)/2T)}{2E_0(\mathbf{p}_1)} \Delta_1^{2M_1}(p_1) p_1^2\, dp_1\, d\mathbf{n}_1, \tag{9}$$

which will now be subjected to analysis and solution. In writing the r.h.s. of this equation, we have replaced the quasiparticle energy $E(\mathbf{p};\eta)$ by $E_0(\mathbf{p};\eta=0) = [\xi^2(p) + D_0^2(\mathbf{p})]^{1/2}$, where $D_0(\mathbf{p})$ is the gap function of the much-studied $^3\mathrm{P}_2$ pairing model in which the tensor coupling between F and P states is ignored. The substitution $E \to E_0$ in the integrals on the right is justified by the small relative size of the quantities $\langle p|V_{13}^2|p_1\rangle$, $\Delta_3^{2M_1}(p_1)$, and $\langle p|V_{31}^2|p_1\rangle$.

A conspicuous feature of the $^3\mathrm{P}_2$ pairing model is the high parametric degeneracy of the spectrum of its solutions. In the case of real solutions, this property has been investigated in detail in Refs. [8,9] in terms of the two ratios $\lambda_1 = D_1^{21}(p_\mathrm{F})\sqrt{6}/D_1^{20}(p_\mathrm{F})$ and $\lambda_2 = D_1^{22}(p_\mathrm{F})\sqrt{6}/D_1^{20}(p_\mathrm{F})$. The degeneracy is reflected in the existence of a set of curves $\lambda_1(\lambda_2)$ in the plane (λ_1, λ_2), upon which all the BCS equations of the $^3\mathrm{P}_2$ problem are satisfied. As we shall see, this degeneracy is essentially lifted in the $^3\mathrm{P}_2$–$^3\mathrm{F}_2$ pairing model where $\eta \neq 0$. A finite set of points (λ_1, λ_2), depending somehow on the η value, replaces the set of solution curves $\lambda_1(\lambda_2)$ of the $^3\mathrm{P}_2$ model.

It is the objective of this article to identify the different solutions of the system (9) and to establish their structure in the realistic case of small η. The analysis is aided by the fact that the parameters $\lambda_1 = f_1(\eta)$ and $\lambda_2 = f_2(\eta)$ are *continuous functions* of the coupling constant η. This property implies that the number of solutions of the $^3\mathrm{P}_2$–$^3\mathrm{F}_2$ pairing problem as well as their structure remains the same no matter how small η is. Consequently, implementation of our program reduces to determination of the functions f_1 and f_2 at $\eta = 0$, i.e., $\lambda_1(\eta = 0)$ and $\lambda_2(\eta = 0)$. It then becomes apparent that the quasiparticle energy $E(\eta)$ may be replaced by E_0 on the left-hand sides of Eqs. (9) as well as on the right, since taking into account the difference $E(\eta)$ and E_0 within (9) cannot, by itself, lift the parametric degeneracy. This conclusion is confirmed in the numerical calculations we have performed.

The nondiagonal integrals on the r.h.s. of Eqs. (9) are rapidly convergent, with the overwhelming contributions coming from momenta adjacent to the Fermi surface. This feature greatly expedites application of the perturbation strategy. For $E(\mathbf{p})$ significantly in excess of the energy gap Δ_F of Eq. (8), the energies $E(\mathbf{p})$ and $|\xi(p)|$ are coincident to high precision, such that the angular integrations in Eqs. (9) yields a null result. Thus, when treating the nondiagonal contributions it is sufficient to know the minor gap components $\Delta_3^{2M}(p)$ at the point $p = p_\mathrm{F}$, which may be efficiently evaluated in terms of the values $D_1^{2M}(p_\mathrm{F})$ (with $M = 0, 1, 2$). In this process, we retain, on the r.h.s. of the last of Eqs. (9), only the dominant contribution containing a large logarithmic factor $L = \ln(\epsilon_\mathrm{F}/\Delta_\mathrm{F})$, where ϵ_F is the Fermi energy. This factor is angle-independent; therefore the respective angular integral is freely evaluated, giving rise to the simple connection

$$\Delta_3^{2M}(p = p_\mathrm{F}) = -L\langle p_\mathrm{F}|V_{13}^2|p_\mathrm{F}\rangle D_1^{2M}(p_\mathrm{F}) = \eta v_\mathrm{F} L D_1^{2M}(p_\mathrm{F}) \simeq \eta D_1^{2M}(p_\mathrm{F}). \tag{10}$$

In obtaining this relation we have employed the equality $1 = v_\mathrm{F} L$, which holds when one keeps only logarithmic contributions. Analogous linear relations are obtained for the other minor components Δ_L^{JM} of the gap function (notably Δ_1^{00} and Δ_1^{1M}).

Insertion of the result (10) into the first of Eqs. (9) leads to the closed system of equations

$$\Delta_1^{2M}(p) + \sum_{M_1} \int\!\!\int \langle p|V_{11}^2|p_1\rangle S_{11}^{2M2M_1}(\mathbf{n}_1) \frac{\tanh(E_0(\mathbf{p}_1)/2T)}{2E_0(\mathbf{p}_1)} \Delta_1^{2M_1}(p_1) p_1^2\, dp_1\, d\mathbf{n}_1$$
$$= \sum_{M_1} \int\!\!\int \langle p|V_{13}^2|p_1\rangle \big[S_{31}^{2M2M_1}(\mathbf{n}_1) + S_{13}^{2M2M_1}(\mathbf{n}_1)\big]$$
$$\times \frac{\tanh(E_0(\mathbf{p}_1)/2T)}{2E_0(\mathbf{p}_1)} \Delta_1^{2M_1}(p_1) p_1^2\, dp_1\, d\mathbf{n}_1, \tag{11}$$

for finding the set of three gap functions $\Delta_1^{2M}(p)$ with $M = 0, 1, 2$.

At this point we invoke the separation method and assert the decomposition [8,9]

$$\Delta_1^{2M}(p) \equiv D_1^{2M} \chi(p) \tag{12}$$

of the gap component into a "universal" shape factor $\chi(p)$ that is *independent* of the magnetic quantum number M and a numerical coefficient D_1^{2M} that embodies the dependence on M. The function $\chi(p)$, normalized by $\chi(p_\mathrm{F}) = 1$, is the solution of a *linear* integral equation. As argued in Refs. [8,9], this decomposition holds to high accuracy in the problem domain under consideration. Accordingly, our problem reduces to the determination of the three key coefficients D_1^{2M}, which obey a set of coupled algebraic equations obtained by setting $p = p_\mathrm{F}$ in Eqs. (11). With $M = 0$, 1, and 2, these equations read

$$D_1^{2M} + v_\mathrm{F} \sum_{M_1} D_1^{2M_1} \int\!\!\int \phi(p) \frac{\tanh(E_0(\mathbf{p})/2T)}{2E_0(\mathbf{p})} S_{11}^{2M2M_1}(\mathbf{n}) \chi(p) p^2\, dp\, d\mathbf{n}$$
$$= \eta v_\mathrm{F} \sum_{M_1} D_1^{2M_1} \int \big[S_{31}^{2M2M_1}(\mathbf{n}) + S_{13}^{2M2M_1}(\mathbf{n})\big] K_0(\mathbf{n})\, d\mathbf{n}, \tag{13}$$

with $\phi(p) \equiv \langle p|V_{11}^2|p_\mathrm{F}\rangle/v_\mathrm{F}$, and

$$K_0(\mathbf{n}) = \int \langle p|V_{13}^2|p_1\rangle \frac{\tanh(E_0(\mathbf{p})/2T)}{2E_0(\mathbf{p})} \chi(p) p^2\, dp. \tag{14}$$

It should be remarked that the integral (14) contains a constant coming from regions lying far from the Fermi surface, but this constant does not contribute to the angular integration on the r.h.s. of Eq. (13).

In the present work, the search for solutions will be confined to those with real coefficients D_1^{2M}. The structure of the phases having complex coefficients D_1^{2M} can be explored and established along the same lines, although the calculations become much more cumbersome. To streamline the task of finding solutions, it is helpful to rewrite Eqs. (13) in terms of the ratios $\lambda_1 = D_1^{21}\sqrt{6}/D_1^{20} = -\Delta_1^{21}\sqrt{6}/D_1^{20}$ and $\lambda_2 = D_1^{22}\sqrt{6}/D_1^{20} = \Delta_1^{22}\sqrt{6}/D_1^{20}$. This step ensures coincidence between the left-hand sides of these equations and their counterparts in the model of pure $^3\mathrm{P}_2$ pairing solved in Ref. [8]. Substitution of the explicit form of $S_{11}^{2M2M_1}(\mathbf{n})$ into Eqs. (13), followed by straightforward algebra, gives a system of three equations

$$\lambda_2 + v_\mathrm{F}\big[\lambda_2(J_0 + J_5) - \lambda_1 J_1 - J_3\big] = \eta v_\mathrm{F} r_2,$$

$$\lambda_1 + v_F\big[-(\lambda_2+1)J_1 + \lambda_1(J_0 + 4J_5 + 2J_3)/4\big] = \eta v_F r_1,$$
$$1 + v_F\big[-(\lambda_2 J_3 + \lambda_1 J_1)/3 + J_5\big] = \eta v_F r_0, \tag{15}$$

for these ratios and the gap value Δ_F. Here, as before [8],

$$J_i = \int\!\!\int f_i(\vartheta,\varphi)\varphi(p)\frac{\tanh(E_0(\mathbf{p})/2T)}{2E_0(\mathbf{p})}\chi(p)\frac{p^2\,dp\,d\mathbf{n}}{4\pi} \tag{16}$$

with $f_0 = 1 - 3z^2$, $f_1 = 3xz/2$, $f_3 = 3(2x^2 + z^2 - 1)/2$, and $f_5 = (1 + 3z^2)/2$ and $z = \cos\vartheta$, $x = \sin\vartheta\cos\varphi$, and $y = \sin\vartheta\sin\varphi$. Among the integrals J_i $(i = 1,\ldots,5)$, only J_5 contains a singular principal term going like $\ln(\epsilon_F/\Delta_F)$. All the other J_i converge close to the Fermi surface, where $E_0(\mathbf{p}) = [\xi^2(p) + D_0^2(\mathbf{n})]^{1/2}$ with

$$D_0^2(\mathbf{n}) = \frac{\Delta_F^2}{2[1+(\lambda_1^2+\lambda_2^2)/3]} \times\Bigg[1 + 3\cos^2\theta + \lambda_2^2\sin^2\theta + \frac{\lambda_1^2}{2}\big(1+\cos^2\theta\big) - 2\lambda_1(1+\lambda_2)\cos\theta\sin\theta\cos\varphi + \frac{1}{2}\big(\lambda_1^2 - 4\lambda_2\big)\sin^2\theta\cos 2\phi\Bigg]. \tag{17}$$

In terms of the coefficients λ_1, λ_2, the right-hand sides of Eqs. (15) read

$$r_2 = \lambda_2 s_{22} + \lambda_1 s_{21} + \sqrt{6}\,s_{20}, \qquad r_1 = \lambda_2 s_{12} + \lambda_1 s_{11} + \sqrt{6}\,s_{10},$$
$$r_0 = \frac{\lambda_2}{\sqrt{6}}s_{02} + \frac{\lambda_1}{\sqrt{6}}s_{01} + s_{00}, \tag{18}$$

where

$$s_{M2} = \int\big[S_{31}^{2M22}(\mathbf{n}) + S_{13}^{2M22}(\mathbf{n}) + S_{31}^{2M2,-2}(\mathbf{n}) + S_{13}^{2M2,-2}(\mathbf{n})\big]K_0(\mathbf{n})\,d\mathbf{n},$$
$$s_{M1} = \int\big[S_{31}^{2M21}(\mathbf{n}) + S_{13}^{2M21}(\mathbf{n}) - S_{31}^{2M2,-1}(\mathbf{n}) - S_{13}^{2M2,-1}(\mathbf{n})\big]K_0(\mathbf{n})\,d\mathbf{n},$$
$$s_{M0} = \int\big[S_{31}^{2M20}(\mathbf{n}) + S_{13}^{2M20}(\mathbf{n})\big]K_0(\mathbf{n})\,d\mathbf{n}. \tag{19}$$

3. Real solutions of the $^3P_2$–$^3F_2$ problem

Eqs. (15) have three familiar *one-component* solutions with definite magnetic quantum numbers $M = 0$, 1, and 2. To uncover the structure and the spectrum of the *multicomponent*, mixed-M solutions of the perturbed problem, a two-step transformation is applied to the system (15). The integral J_5 introduces the gap value Δ_F into the description, but it is irrelevant to the phase structure. As a first step, we combine Eqs. (15) so as to eliminate terms involving J_5 from the first pair and, at the same time, reduce the number of the J_i integrals in each equation to two. The resulting equations are

$$(\lambda_2+1)\big[3\lambda_1(\lambda_2+1)J_0 - 2\big(\lambda_1^2 - 2\lambda_2^2 + 6\big)J_1\big] = \eta B_1,$$
$$(\lambda_2+1)\big[\big(\lambda_1^2 - 4\lambda_2\big)J_1 + \lambda_1(\lambda_2+1)J_3\big] = \eta B_2, \tag{20}$$

with

$$B_1 = 2\lambda_1(2\lambda_2+3)r_2 - 4\big(\lambda_2^2-3\big)r_1 - 6\lambda_1(\lambda_2+2)r_0,$$
$$B_2 = -\lambda_1 r_2 + 4\lambda_2 r_1 - 3\lambda_1\lambda_2 r_0. \tag{21}$$

Two cases are to be distinguished. The first corresponds to $\lambda_2 = -1$, a particular solution of the pure $^3P_2$ pairing problem [8]. In this case, the left-hand sides of Eqs. (20) vanish identically, and hence so must their right-hand sides, leading to the single restriction

$$\lambda_1 r_2(\lambda_1;-1) + 4r_1(\lambda_1;-1) - 3\lambda_1 r_0(\lambda_1;-1) = 0. \tag{22}$$

As will be seen, this condition is satisfied at *any* λ_1. Therefore, the particular solution $\lambda_2 = -1$ found in the pure $^3P_2$ problem survives intact when the $^3F_2$ coupling is switched on.

Let us now assume $\lambda_2 \neq -1$ and proceed to the second step. Following Ref. [8], we perform a rotation

$$\begin{cases} z = t\cos\beta + u\sin\beta, \\ x = -t\sin\beta + u\cos\beta, \end{cases} \tag{23}$$

with the objective of removing the integral J_1 from Eqs. (20). To this end, the parameter $\zeta = \tan\beta$ is taken as a root of the quadratic equation

$$\zeta^2 + \frac{3-\lambda_2}{\lambda_2}\zeta - 1 = 0. \tag{24}$$

The integrals J_i transform according to

$$J_0 \to J_0\left(\cos^2\beta - \frac{1}{2}\sin^2\beta\right) - J_3\sin^2\beta,$$
$$J_1 \to -\frac{3}{4}J_0\sin^2\beta + J_3\left(\cos^2\beta + \frac{1}{2}\sin^2\beta\right),$$
$$J_1 \to \left(\frac{3}{4}J_0 + \frac{1}{2}J_3\right)\sin\beta\cos\beta. \tag{25}$$

Substitution of the transformed integrals into Eqs. (20) yields

$$(\lambda_2+1)[A_1J_0 + A_2J_3] = \eta B_1,$$
$$(\lambda_2+1)[A_1J_0 + A_2J_3] = -2\eta B_2, \tag{26}$$

with

$$A_1 = \frac{3}{2}\lambda_1(1+\lambda_2)\big(2-\zeta^2\big) - \frac{3}{2}\big(\lambda_1^2 - 2\lambda_2^2 + 6\big)\zeta,$$
$$A_2 = -3\lambda_1(1+\lambda_2)\zeta^2 - \big(\lambda_1^2 - 2\lambda_2^2 + 6\big)\zeta. \tag{27}$$

(Some details of this step are provided in Refs. [8,13].)

The left-hand members of the two equations (26) are seen to be identical. In fact, the universalities of pure $^3P_2$ pairing revealed in Ref. [8] stem from this key property. The solutions of the restricted problem derived from Eqs. (26) at $\eta \equiv 0$ fall into two groups composed of states that are degenerate in energy. This remarkable feature is independent

of temperature, density, and details of the in-medium interaction. There is an upper (i.e., higher-energy) group consisting of states whose angle-dependent order parameters have nodes and a lower group without nodes (cf. Ref. [18]). In addition to the energy degeneracies, the multicomponent pairing solutions, which obey the relation

$$\left(\lambda_1^2 - 2\lambda_2^2 - 6\lambda_2\right)\left(\lambda_1^2 + 2 - 2\lambda_2\right) = 0, \tag{28}$$

manifest a parametric degeneracy with respect to the coefficient ratios λ_1 and λ_2, as they in general define *curves* rather than *points* in the (λ_1, λ_2) plane.

Among solutions of the ${}^3\mathrm{P}_2$–${}^3\mathrm{F}_2$ pairing model there exist some for which B_1 and B_2 in Eqs. (26) vanish simultaneously at a certain set of parameters λ_1 and λ_2 satisfying Eqs. (28). Indeed, consider the set of values

$$\lambda_1 = 0; \qquad \lambda_2 = \pm 1, \pm 3, \tag{29}$$

which determine two-component solutions of the pure ${}^3\mathrm{P}_2$ pairing problem [8]. In these cases, it may be observed from Eqs. (21) and (18) that

$$\begin{aligned} &B_1(\lambda_1 = 0, \lambda_2) \sim B_2(\lambda_1 = 0, \lambda_2) \sim r_1(\lambda_1 = 0, \lambda_2) \\ &\quad = \lambda_2 s_{12}(\lambda_1 = 0, \lambda_2) + \sqrt{6}\, s_{10}(\lambda_1 = 0, \lambda_2), \end{aligned} \tag{30}$$

where $s_{12}(\lambda_1 = 0, \lambda_2)$ and $s_{10}(\lambda_1 = 0, \lambda_2)$ are defined by Eqs. (19). As seen from Eq. (17), the quantities $D_0(\lambda_1 = 0, \lambda_2; \mathbf{n})$ and $K_0(\lambda_1 = 0, \lambda_2; \mathbf{n})$ are even functions of $\cos\varphi$ [6,8], while both $S_{31}^{2122}(\mathbf{n}) + S_{13}^{2122}(\mathbf{n}) + S_{31}^{212,-2}(\mathbf{n}) + S_{13}^{212,-2}(\mathbf{n})$ and $S_{31}^{2120}(\mathbf{n}) + S_{13}^{2120}(\mathbf{n})$ appear to be linear in $\cos\varphi$ (for details, refer to Appendix A). As a result, both the matrix elements $s_{12}(\lambda_1 = 0, \lambda_2)$ and $s_{10}(\lambda_1 = 0, \lambda_2)$ vanish identically when the integration over φ is performed. Hence both of the quantities B_1 and B_2 turn out to be zero, and we find that the parameter values (29) define a discrete set of valid two-component solutions for the ${}^3\mathrm{P}_2$–${}^3\mathrm{F}_2$ pairing problem as well as for the pure ${}^3\mathrm{P}_2$ case. No other two-component solutions of the former problem have been found in numerical calculations.

Continuing our exploration, suppose that B_1 and B_2 do not vanish. Equating the right-hand members of Eqs. (26) in the $\eta \to 0$ limit, we then obtain an *additional* relation between the parameters $\lambda_1(\eta = 0)$ and $\lambda_2(\eta = 0)$ similar to (22), namely,

$$\lambda_1 r_2(\lambda_1, \lambda_2) - (\lambda_2 - 3) r_1(\lambda_1, \lambda_2) - 3\lambda_1 r_0(\lambda_1, \lambda_2) = 0, \tag{31}$$

the quantities r_M being defined by Eqs. (18). Inserting the explicit expressions for the r_M, this auxiliary condition can be recast as

$$\begin{aligned} &G(\lambda_1, \lambda_2) \\ &\quad = \int K_0(x, y, z; \lambda_1, \lambda_2) \Psi(x, y, z; \lambda_2) \delta\left(1 - x^2 - y^2 - z^2\right) \frac{dx\, dy\, dz}{2\pi} = 0, \end{aligned} \tag{32}$$

where $\Psi(x, z; \lambda_1, \lambda_2) \equiv \lambda_1 R_2(x, z) - (\lambda_2 - 3) R_1(x, z) - 3\lambda_1 R_0(x, z)$ and the quantities R_k are given in the appendix. Substituting for the R_k, we obtain

$$\begin{aligned} &\Psi(x, z; \lambda_1, \lambda_2) \\ &\quad = 14\lambda_1 \left[5(\lambda_2 + 3) z^4 - 10\lambda_2 x^4 + 15(\lambda_2 - 3) x^2 z^2 + 6(\lambda_2 + 1)\left(x^2 - z^2\right)\right] \\ &\qquad + 70\left[(\lambda_2 - 3)(\lambda_2 + 3) + 2\lambda_1^2\right] x z^3 + 70\left[2\lambda_2(\lambda_2 - 3) - 2\lambda_1^2\right] x^3 z \\ &\qquad - 96(\lambda_2 - 3)(\lambda_2 + 1) x z. \end{aligned} \tag{33}$$

The relation (32) supplements the spectral condition (28). As a direct consequence, the strong parametric degeneracy inherent in pure $^3P_2$ pairing is lifted in the case of $^3P_2$–$^3F_2$ pairing. With the exception of the straight-line solution $\lambda_2 = 1$ noted above, the solutions of the problem are now represented by a set of *isolated* points in the (λ_1, λ_2) plane.

The system formed by Eqs. (28) and (31) is amenable to analytic solution. We begin the search for solutions of Eq. (32) with the particular solution $(\lambda_1, \lambda_2 = -1)$ of the pure $^3P_2$ pairing problem. In this case,

$$\begin{aligned}
&\Psi(x, y, z; \lambda_1, \lambda_2 = -1) \\
&\quad \sim z^4 + x^4 - 6x^2z^2 \\
&\quad = 8z^4 - 3\big(1 - y^2\big)^2 - 4\big(1 - y^2\big)\big(2z^2 - 1 + y^2\big),
\end{aligned} \tag{34}$$

while, as seen from (17), the gap function $D_0^2(\lambda_2 = -1; \mathbf{n})$ depends only on the single variable y:

$$D_0^2(x, y, z; \lambda_1, \lambda_2 = -1) \sim \frac{3}{2}\big(x^2 + z^2\big) = \frac{3}{2}\big(1 - y^2\big). \tag{35}$$

Since the integrals

$$\int\limits_{-\sqrt{1-y^2}}^{\sqrt{1-y^2}} \frac{8z^4 - 3(1-y^2)^2}{\sqrt{1-y^2-z^2}}\,dz \quad \text{and} \quad \int\limits_{-\sqrt{1-y^2}}^{\sqrt{1-y^2}} \frac{2z^2 - 1 + y^2}{\sqrt{1-y^2-z^2}}\,dz \tag{36}$$

both vanish, the integral $G(\lambda_1, \lambda_2 = -1)$ also vanishes at any λ_1. Accordingly, the degenerate solution $\lambda_2 = -1$ of the uncoupled $^3P_2$ pairing problem survives when the $^3F_2$ channel is involved.

In search of other solutions, we again make use of the transformation (23), applying it now to the whole integrand of Eq. (32). As found in Ref. [8], the gap function D_0 reduces to a function of the single variable t under such a transformation; hence the same property holds for the factor K_0 in Eq. (32), which is defined as a functional of D_0 by Eq. (14). To ascertain how the factor Ψ is transformed, let us write down the results of the transformation for simple terms entering this function. In implementing the transformation we omit odd-power terms u and u^3, which do not contribute to the integral (32). One obtains

$$\begin{aligned}
&x^4 \to t^4 \sin^4\beta + u^4 \cos^4\beta + 6t^2u^2 \sin^2\beta \cos^2\beta, \\
&z^4 \to t^4 \cos^4\beta + u^4 \sin^4\beta + 6t^2u^2 \sin^2\beta \cos^2\beta, \\
&x^2z^2 \to t^4 \sin^2\beta \cos^2\beta + u^4 \sin^2\beta \cos^2\beta \\
&\qquad\quad + t^2u^2\big(\sin^4\beta + \cos^4\beta - 4\sin^2\beta \cos^2\beta\big), \\
&xz^3 \to u^4 \sin^3\beta \cos\beta - t^4 \cos^3\beta \sin\beta + 3t^2u^2\big(\cos^3\beta \sin\beta - \sin^3\beta \cos\beta\big), \\
&x^3z \to u^4 \cos^3\beta \sin\beta - t^4 \sin^3\beta \cos\beta - 3t^2u^2\big(\cos^3\beta \sin\beta - \sin^3\beta \cos\beta\big), \\
&x^2 - z^2 \to \big(t^2 - u^2\big)\big(\cos^2\beta - \sin^2\beta\big).
\end{aligned} \tag{37}$$

After inserting these relations into the formula (33) for Ψ, simple algebra yields

$$\Psi(t,u;\lambda_1,\lambda_2) = \bigl(1+\zeta^2\bigr)^{-2}\bigl[Uu^4 + Tt^4 + V\bigl(u^2-t^2\bigr) + Wu^2t^2\bigr], \tag{38}$$

where

$$\begin{aligned} U(\lambda_1,\lambda_2) = 70\Bigl\{&\lambda_1(\lambda_2+3)\zeta^4 + \bigl[(\lambda_2-3)(\lambda_2+3)+2\lambda_1^2\bigr]\zeta^3 \\ &+ 3\lambda_1(\lambda_2-3)\zeta^2 + \bigl[2\lambda_2(\lambda_2-3)-2\lambda_1^2\bigr]\zeta - 2\lambda_1\lambda_2\Bigr\}, \end{aligned} \tag{39}$$

$$\begin{aligned} T(\lambda_1,\lambda_2) = 70\Bigl\{&-2\lambda_1\lambda_2\zeta^4 - \bigl[2\lambda_2(\lambda_2-3)-2\lambda_1^2\bigr]\zeta^3 + 3\lambda_1(\lambda_2-3)\zeta^2 \\ &- \bigl[(\lambda_2-3)(\lambda_2+3)+2\lambda_1^2\bigr]\zeta + \lambda_1\bigl(\lambda_2+3\bigr)\Bigr\}, \end{aligned} \tag{40}$$

$$\begin{aligned} V(\lambda_1,\lambda_2) = 24\Bigl[&7\lambda_1(\lambda_2+1)\bigl(1+\zeta^2\bigr)\bigl(1-\zeta^2\bigr) \\ &- 8(\lambda_2-3)(\lambda_2+1)\bigl(1+\zeta^2\bigr)\zeta\Bigr], \end{aligned} \tag{41}$$

$$\begin{aligned} W(\lambda_1,\lambda_2) = 210\Bigl\{&2\lambda_1(\lambda_2+3)\zeta^2 - 4\lambda_1\lambda_2\zeta^2 + \lambda_1(\lambda_2-3)\bigl(\zeta^4+1-4\zeta^2\bigr) \\ &+ \bigl[(\lambda_2-3)(\lambda_2+3)+2\lambda_1^2\bigr]\bigl(\zeta-\zeta^3\bigr) \\ &+ \bigl[2\lambda_2(\lambda_2-3)-2\lambda_1^2\bigr]\bigl(\zeta^3-\zeta\bigr)\Bigr\}. \end{aligned} \tag{42}$$

These results can be simplified slightly by employing the connection $\lambda_1(\zeta^2-1) = (\lambda_2-3)\zeta$, and one finally arrives at

$$\begin{aligned} U(\lambda_1,\lambda_2) = 70\bigl[&\lambda_1(\lambda_2+3)\zeta^4 + 5\lambda_1(\lambda_2-3)\zeta^2 - 2\lambda_1\lambda_2 \\ &+ (\lambda_2-3)(\lambda_2+3)\zeta^3 + 2\lambda_2(\lambda_2-3)\zeta\bigr], \end{aligned} \tag{43}$$

$$\begin{aligned} T(\lambda_1,\lambda_2) = 70\bigl[&\lambda_1(\lambda_2+3) + 5\lambda_1(\lambda_2-3)\zeta^2 - 2\lambda_1\lambda_2\zeta^4 \\ &- (\lambda_2-3)(\lambda_2+3)\zeta - 2\lambda_2(\lambda_2-3)\zeta^3\bigr], \end{aligned} \tag{44}$$

$$\begin{aligned} V(\lambda_1,\lambda_2) &= 180\lambda_1(\lambda_2+1)\bigl(1-\zeta^4\bigr), \\ W(\lambda_1,\lambda_2) &= 420\lambda_1(\lambda_2-3)\bigl(\zeta^4-6\zeta^2+1\bigr). \end{aligned} \tag{45}$$

The auxiliary integrals

$$\begin{aligned} I_0 &= \int\limits_{-\sqrt{1-t^2}}^{\sqrt{1-t^2}} \frac{du}{\sqrt{1-t^2-u^2}} = \pi, \\ I_2 &= \int\limits_{-\sqrt{1-t^2}}^{\sqrt{1-t^2}} \frac{u^2\,du}{\sqrt{1-t^2-u^2}} = \frac{\pi(1-t^2)}{2}, \end{aligned} \tag{46}$$

and

$$I_4 = \int\limits_{-\sqrt{1-t^2}}^{\sqrt{1-t^2}} \frac{u^4\,du}{\sqrt{1-t^2-u^2}} = \frac{3\pi(1-t^2)^2}{8} \tag{47}$$

are helpful in completing the evaluation of $G(\lambda_1, \lambda_2)$ by integration over the new variables. The integrals I_0, I_2, and I_4 are related by

$$I_4 = \frac{3}{4}\big(1-t^2\big)I_2 = \frac{3}{8}\big(1-t^2\big)^2 I_0, \qquad I_2 = \frac{1}{2}\big(1-t^2\big)I_0. \tag{48}$$

Using these connections, one can easily verify that integration of the combinations $8u^4 - 3(1-t^2)^2$ and $2u^2 - 1 + t^2$ over u gives zero. It follows then that if we make the following replacements

$$u^2 \to \frac{1}{2}\big(1-t^2\big), \qquad u^4 \to \frac{3}{8}\big(1-t^2\big)^2 \tag{49}$$

in Eq. (33), the new function

$$\begin{aligned}\Psi'(t,\lambda_1,\lambda_2) = \frac{1}{8(1+\zeta^2)^2}\Big\{&\big[3U(\lambda_1,\lambda_2) + 8T(\lambda_1,\lambda_2) - 4W(\lambda_1,\lambda_2)\big]t^4 \\ &- \big[6U(\lambda_1,\lambda_2) + 12V(\lambda_1,\lambda_2) - 4W(\lambda_1,\lambda_2)\big]t^2 \\ &+ 3U(\lambda_1,\lambda_2) + 4V(\lambda_1,\lambda_2)\Big\}\end{aligned} \tag{50}$$

will guarantee the same result as given by Ψ upon integration of Eq. (32). For this integral to vanish identically, with the function $K_0(t)$ regarded as arbitrary, the coefficients of all powers of t in the function Ψ' must be zero:

$$\begin{cases} 3U(\lambda_1,\lambda_2) + 8T(\lambda_1,\lambda_2) - 4W(\lambda_1,\lambda_2) = 0, \\ 3U(\lambda_1,\lambda_2) + 6V(\lambda_1,\lambda_2) - 2W(\lambda_1,\lambda_2) = 0, \\ 3U(\lambda_1,\lambda_2) + 4V(\lambda_1,\lambda_2) = 0. \end{cases} \tag{51}$$

This system reduces to the chain of equations

$$T(\lambda_1,\lambda_2) = V(\lambda_1,\lambda_2) = W(\lambda_1,\lambda_2) = -\frac{3}{4}U(\lambda_1,\lambda_2), \tag{52}$$

where λ_1 and λ_2 are to satisfy the relation (28). It can be proved that to determine all solutions of this set it is sufficient to solve the equation

$$V(\lambda_1,\lambda_2) = W(\lambda_1,\lambda_2), \tag{53}$$

which has the explicit form

$$3(\lambda_2+1)\big(1-\zeta^4\big) = 7(\lambda_2-3)\big(\zeta^4 - 6\zeta^2 + 1\big), \tag{54}$$

and then to verify that the other equalities in (52) hold for these solutions.

To solve Eq. (54), consider the first branch of Eq. (28),

$$\lambda_1^2 = 2\lambda_2^2 + 6\lambda_2, \tag{55}$$

for which

$$\zeta = \tan\beta = \frac{2\lambda_2}{\lambda_1}. \tag{56}$$

Then Eq. (54) is recast to

$$(\lambda_2 - 3)\left(5\lambda_2^2 + 24\lambda_2 - 9\right) = 0. \tag{57}$$

One root of this equation is obviously $\lambda_2 = 3$, which corresponds to $\lambda_1 = 6$. Another pair of roots is given by

$$\lambda_2 = \frac{3}{5}\left(\pm\sqrt{21} - 4\right) \approx 0.350, -5.150, \tag{58}$$

yielding, respectively,

$$\lambda_1 = \frac{3}{5}\sqrt{2\left(17 \mp 3\sqrt{21}\right)} \approx 1.530,\ 4.705. \tag{59}$$

Now consider the second branch of Eq. (28),

$$\lambda_2 = \frac{\lambda_1^2}{2} + 1, \tag{60}$$

with

$$\zeta = -\frac{2}{\lambda_1}. \tag{61}$$

In this case, Eq. (54) becomes

$$(\lambda_2 - 3)\left(\lambda_2^2 - 26\lambda_2 + 29\right) = 0. \tag{62}$$

Its roots are $(\lambda_2, \lambda_2) = (3, 2)$ and

$$\lambda_2 = 13 \mp 2\sqrt{35} \approx 1.168,\ 24.83,$$
$$\lambda_1 = 2\sqrt{6 \mp \sqrt{35}} \approx 0.579,\ 6.904. \tag{63}$$

Insertion of these solutions into other (52) results in a chain of identities, as required.

4. Phases of $^3P_2$–$^3F_2$ pairing

The set of solutions of the $^3P_2$–$^3F_2$ pairing problem revealed by the above analysis is depicted in Fig. 1 and cataloged in Table 1.

Fig. 1 refers to the multicomponent solutions and represents them by their coordinates (λ_1, λ_2) in the two-dimensional parameter space. Only the right half of the $\lambda_1 - \lambda_2$ plane is plotted, because the pairing energies are independent of the sign of λ_1. The most important message of this figure is that (with the exception previously noted) the solution curves that represent parametrically degenerate solutions of the $^3P_2$ problem shrink to discrete points as the degeneracy is lifted by the perturbation that admixes the $^3F_2$ channel.

The solutions (which correspond to pairing states and ultimately to superfluid phases) divide into two categories: those whose order parameters contain nodes and those whose

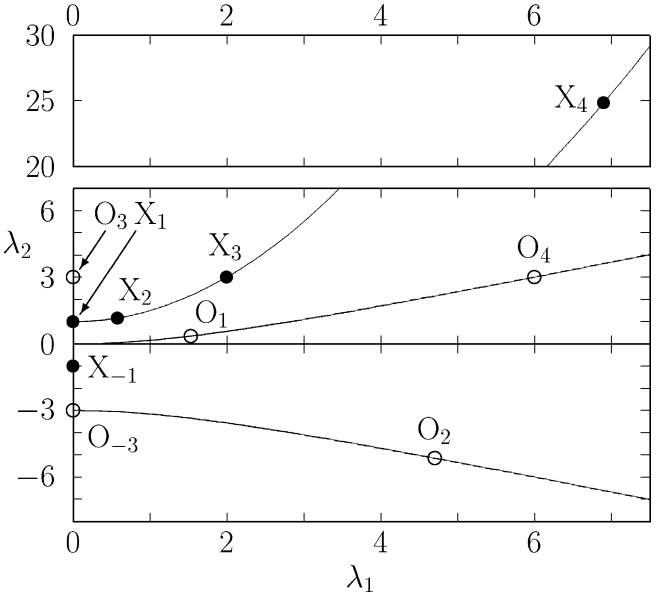

Fig. 1. Parameter sets (λ_1, λ_2) defining the multicomponent solutions of the $^3P_2$–$^3F_2$ pairing problem. Solution curves or points of the pure, uncoupled $^3P_2$ problem are identified with an open circle (or a filled circle) according as their order parameters are nodeless (or display nodes).

Table 1
Identification of the thirteen solutions (or superfluid phases) of the $^3P_2$ pairing model, in terms of the parameters λ_1 and λ_2 defining their magnetic content, and in terms of their nodeless (states labeled O) or nodal (states labeled X) character

Phase	λ_1		λ_2
$O_{M=0}$		$M=0$	
$X_{M=1}$		$M=1$	
$X_{M=2}$		$M=2$	
O_3	0		3
O_{-3}	0		-3
X_1	0		1
X_{-1}	0		-1
O_1	$\frac{3}{5}\sqrt{2(17-3\sqrt{21})}$		$\frac{3}{5}(\sqrt{21}-4)$
O_2	$\frac{3}{5}\sqrt{2(17+3\sqrt{21})}$		$-\frac{3}{5}(\sqrt{21}+4)$
O_4	6		3
X_2	$2\sqrt{6-\sqrt{35}}$		$13-2\sqrt{35}$
X_3	2		3
X_4	$2\sqrt{6+\sqrt{35}}$		$13+2\sqrt{35}$

order parameters are nodeless. It is convenient to identify the nodal states with the symbol X and the nodeless states with the symbol O.

First there are the three well-known "one-component" solutions, belonging to magnetic quantum numbers $M = \pm 2$, $M = \pm 1$, and $M = 0$, respectively. In addition, we have established the existence of ten multicomponent solutions that mix states with different values of $|M|$. These are comprised of five nodeless solutions and five exhibiting nodes.

The five nodeless multicomponent solutions O_k include:

(i) Two two-component solutions denoted $O_{\pm 3}$, which are *identical* to the "particular" solutions found in the pure $^3P_2$ case having $\lambda_1 = 0$ and $\lambda_2 = \pm 3$.
(ii) Three three-component solutions associated with the branch (55) of Eq. (28). Two of these, denoted O_1 and O_4, derive respectively from the upper root of the pair (58) and the root $\lambda_2 = 3$. The third, named O_2, derives from the lower root of the pair (58).

The five nodal solutions X_k consist of:

(i) Two two-component solutions $X_{\pm 1}$ that are identical to the "particular" solutions found in the pure $^3P_2$ problem having $\lambda_1 = 0$ and $\lambda_2 = \pm 1$.
(ii) Three three-component solutions associated with the branch (60) of Eq. (28). The solutions X_2 and X_4 derive, respectively, from the lower and upper roots of the pair (63), while X_3 derives from the root $\lambda_2 = 3$.

Appealing to continuity in the parameter η, it may be expected that the general features of the spectrum of solutions delineated by the perturbative analysis will persist even when η is not especially small.

5. Discussion

In the present article, we have employed the separation method of Ref. [8] to derive, from the system of nonlinear BCS integral equations for the components $\Delta_L^{JM}(\mathbf{p})$ of the gap function, a set of nonlinear algebraic equations for the coefficients specifying the angular structure of the superfluid states of interest. Based on this stratagem, we have been able to find all the real solutions of the $^3P_2$–$^3F_2$ pairing problem in the regime of vanishingly small η. Their salient feature is a remarkable independence of the temperature T and of any details of the interaction $\mathcal{V}$. In principle, the full collection of complex solutions can also be obtained along the same lines, but the calculations become much more cumbersome.

It must be noted that the status of the $^3P_2$–$^3F_2$ pairing model, in which contributions from $^3P_2 \to {}^3P_0$ or $^3P_2 \to {}^3P_1$ transitions are assumed to be unimportant, is somewhat vulnerable. This assumption should be a safe one in the low-density regions of a neutron star. However, it may not hold in the denser core region, where (i) the cancellation between different contributions to the P-wave central component of the scattering amplitude becomes questionable and (ii) the amplification of the tensor force due to the pion-exchange renormalization [15] becomes pronounced. These effects, which increase with

density, may overwhelm the spin–orbit component in the effective pairing interaction, whose strength depends only mildly on density. The $^3P_0$ pairing channel would then take command and give rise to a superfluid state analogous to the B-state of liquid ^{3}He. In the less challenging situation where $^3P_2 \to {}^3P_0$ transitions can be described within perturbation theory, their effects reduce to a renormalization of the matrix elements s_{MM_1}, which acquire an additional term of the form

$$\delta s_{MM_1} \sim \int S_{11}^{2M00}(\mathbf{n})\, K_0(\mathbf{n})\, d\mathbf{n} \int S_{11}^{002M_1}(\mathbf{n})\, K_0(\mathbf{n})\, d\mathbf{n}. \tag{64}$$

An analogous modification occurs when contributions from $^3P_2 \to {}^3P_1$ transitions are taken into account perturbatively.

In short, the introduction of new transitions among two-body states results in the mixing of components having different values of total angular momentum J. This effect depends very strongly on the proximity to the critical temperature T_c. It is well known that in the immediate vicinity of T_c, all the BCS equations decouple; hence the various phases that appear may be classified according to the quantum number J. These considerations apply as well to superfluid ^{3}He. The magnetic dipole interaction between the ^{3}He atoms—which is responsible for such a phase separation close to T_c—triggers the planar state with $J = 1$ [1,20]. This result is unaffected by strong-coupling corrections.

Let us now turn to a more detailed analysis of the impact of transitions between pairing states. We start with the two-component solutions (29), namely, $\lambda_1 = 0$, $\lambda_2 = \pm 1, \pm 3$, and recall that in the $^3P_2$–$^3F_2$ model, both of the quantities $B_1(\lambda_1 = 0)$ and $B_2(\lambda_1 = 0)$, which behave as $r_1(\lambda_1 = 0)$, vanish identically. As will now be argued, this property holds in an extended version that allows for transitions between states with different J values. Upon setting $\lambda_1 = 0$ in Eqs. (21) and (18) determining B_1 and B_2, there apparently remains a single term containing $r_1(\lambda_1 = 0, \lambda_2) = \lambda_2 \delta s_{12}(\lambda_1 = 0, \lambda_2) + \sqrt{6}\, \delta s_{10}(\lambda_1 = 0, \lambda_2)$. But upon closer inspection of the integrands in (64), this term is also found to vanish. According to Eq. (14), $K_0(\lambda_1 = 0, \mathbf{n})$ is an even function of $\cos\varphi$ independently of λ_2, while $S_{11}^{2100}(\mathbf{n})$, the explicit form of which is given in the appendix, is an odd function of $\cos\varphi$. Nullification of the respective integrals therefore occurs upon integration over φ. Consequently, the equality $B_1 = B_2 = 0$ applies even when the transitions $^3P_2 \to {}^3P_1$ are incorporated into the description. It follows that the spectrum (29) of the two-component solutions of the $^3P_2$–$^3F_2$ pairing model endures upon inclusion of the $^3P_2 \to {}^3P_0$ and $^3P_2 \to {}^3P_1$ transitions.

The opposite situation is encountered when one considers the particular solution of the $^3P_2$–$^3F_2$ pairing model defined by the straight line $\lambda_2 = -1$. The single point $\lambda_1 = 0$, $\lambda_2 = -1$ of this line does survive as a solution of the pairing problem, but the other points do not. To confirm this assertion, we first observe that in Eq. (22), contributions from the corrected values of r_2 and r_0 are proportional to λ_1 and hence vanish provided $\lambda_1 = 0$; further, as seen from Eqs. (18), the corrected value of $r_1(\lambda_1 = 0)$ is zero, since contributions from the terms of Eq. (64) vanish at $\lambda_1 = 0$. To reveal other viable points on the straight line, one looks for the zeroes of the terms introduced in the l.h.s. of Eq. (22) by $^3P_2 \to {}^3P_0$ and $^3P_2 \to {}^3P_1$ transitions. Direct calculation shows that the term corresponding to the $^3P_2 \to {}^3P_1$ transition vanishes identically on the line $\lambda_2 = -1$, while that for the $^3P_2 \to {}^3P_0$ transition is proportional to $\lambda_1 J_0^2$, where the integral J_0 is given

by Eq. (16). It can be checked that this expression has no new zeroes on the straight line $\lambda_2 = -1$ in addition to the point $\lambda_1 = 0$.

Close inspection reveals that the revised locations of the other solutions found above depend on the matrix elements of the interaction $\mathcal{V}$; if the ratio $\langle p_F|V_{11}^{J\neq 2}|p_F\rangle/\langle p_F|V_{13}^2|p_F\rangle$ is small then the shifts from the old positions are also small. Naturally it is of interest to trace the trajectories of solutions as this ratio is varied, thereby exploring the phenomenon of triplet pairing in the continuum of cases from that of dense neutron matter to that of superfluid ^{3}He. This investigation will be a subject of future work.

Our method is to be compared with Ginzburg–Landau (GL) theory, which is generally regarded as the standard technique for mapping the spectrum of the phases of systems with triplet pairing. In the GL method, the search for diverse phases is based on the construction of a suitable free energy functional up to terms of fourth (or even sixth) power in the gap value Δ. This approach allows one to simultaneously evaluate the splitting between the different phases and efficiently determine the phase diagram. Another advantage of the GL procedure resides in the facility of including strong-coupling corrections [19] arising from the dependence of the effective interaction $\mathcal{V}$ on the gap value, which becomes important close to the critical temperature T_c. Unfortunately, the GL method fails when the temperature T is significantly different from T_c. Its application to the phase-spectrum problem makes sense only if the phase structure of superfluid neutron matter is independent of T. However, special conditions must be met for this to be true in the face of the explicit appearance of the factor $\tanh(E/2T)$ in the set of BCS equations, and the explication of these conditions is impossible within the GL approach itself. Our method is free of these shortcomings. It is equally reliable close to T_c and at $T = 0$. Moreover, the incorporation of strong-coupling corrections reduces to the insertion of new terms in $\mathcal{V}$ that depend on Δ itself; if this dependence is appropriately specified, no further hurdles must be overcome to fully elucidate the triplet superfluid phase diagram.

In a sequel to this paper, we shall report the findings of a quantitative treatment of the transitions between the phases arising in the $^3P_2$–$^3F_2$ model and construct the corresponding superfluid phase diagram of dense neutron matter. This task requires significant numerical effort beyond the analytic developments of the present work.

Acknowledgement

This research was supported in part by the US National Science Foundation under Grant No. PHY-0140316, by the McDonnell Center for the Space Sciences at Washington University, and by Grant No. 00-15-96590 from the Russian Foundation for Basic Research (V.A.K. and M.V.Z.). J.W.C. also acknowledges support received from Fundaç ao Luso-Americana para o Desenvolvimento (FLAD) and from Fundaç ao para a Ciência e a Technologia (FCT) for his participation in Madeira Math Encounters XXIII at the University of Madiera, where some of this work was done. He thanks Professor Ludwig Streit and his colleagues for the generous hospitality extended by the Centro de Ciências Mathemáticas.

Appendix A. Explicit formulas for matrix elements

To find analytic solutions of the system (3), explicit formulas for the set of matrix elements

$$
\begin{aligned}
S_{LL_1}^{JMJ_1M_1}(\mathbf{n}) \;=\; & (-1)^{M+1+(L-L_1+K)/2}\frac{1}{4\pi} \\
& \times \sum_{K\kappa} \sqrt{(2K+1)(2J+1)(2J_1+1)(2L+1)(2L_1+1)} \\
& \times \begin{pmatrix} K & L & L_1 \\ 0 & 0 & 0 \end{pmatrix} \begin{pmatrix} K & J_1 & J \\ \kappa & M_1 & -M \end{pmatrix} \begin{Bmatrix} K & J_1 & J \\ 1 & L & L_1 \end{Bmatrix} \\
& \times (-1)^{(\kappa+|\kappa|)/2} \mathcal{P}_{K\kappa}(\vartheta,\varphi) e^{-i\kappa\varphi}
\end{aligned} \tag{A.1}
$$

are needed, where the $\mathcal{P}_{K\kappa}(\vartheta,\varphi)$ are associated Legendre polynomials. Lengthy algebra involving $3j$- and $6j$-symbols yields

$$
\left(S_{13}^{2020} + S_{31}^{2020}\right) = \frac{1}{7\pi}\sqrt{\frac{3}{2}}\left(-\frac{105}{4}\cos^4\vartheta + 21\cos^2\vartheta - \frac{7}{4}\right), \tag{A.2}
$$

$$
\left(S_{13}^{2021} + S_{31}^{2021}\right) = \frac{1}{7\pi}\left(12\sin\vartheta\cos\vartheta - \frac{105}{4}\sin\vartheta\cos^3\vartheta\right)e^{i\varphi}, \tag{A.3}
$$

$$
\left(S_{13}^{202,-1} + S_{31}^{202,-1}\right) = -\frac{1}{7\pi}\left(12\sin\vartheta\cos\vartheta - \frac{105}{4}\sin\vartheta\cos^3\vartheta\right)e^{-i\varphi}, \tag{A.4}
$$

$$
\left(S_{13}^{2022} + S_{31}^{2022}\right) = \frac{1}{7\pi}\left(\frac{21}{8}\sin^2\vartheta - \frac{105}{8}\sin^2\vartheta\cos^2\vartheta\right)e^{2i\varphi}, \tag{A.5}
$$

$$
\left(S_{13}^{202,-2} + S_{31}^{202,-2}\right) = \frac{1}{7\pi}\left(\frac{21}{8}\sin^2\vartheta - \frac{105}{8}\sin^2\vartheta\cos^2\vartheta\right)e^{-2i\varphi}, \tag{A.6}
$$

$$
\left(S_{13}^{2120} + S_{31}^{2120}\right) = \frac{1}{7\pi}\left(12\sin\vartheta\cos\vartheta - \frac{105}{4}\sin\vartheta\cos^3\vartheta\right)e^{-i\varphi}, \tag{A.7}
$$

$$
\left(S_{13}^{2121} + S_{31}^{2121}\right) = \frac{1}{7\pi}\sqrt{\frac{3}{2}}\left(\frac{35}{2}\cos^4\vartheta - \frac{63}{4}\cos^2\vartheta + \frac{7}{4}\right), \tag{A.8}
$$

$$
\left(S_{13}^{212,-1} + S_{31}^{212,-1}\right) = -\frac{1}{7\pi}\sqrt{\frac{3}{2}}\left(\frac{35}{2}\cos^4\vartheta - \frac{77}{4}\cos^2\vartheta + \frac{7}{4}\right)e^{-2i\varphi}, \tag{A.9}
$$

$$
\left(S_{13}^{2122} + S_{31}^{2122}\right) = \frac{1}{7\pi}\sqrt{\frac{3}{2}}\left(-\frac{9}{4}\sin\vartheta\cos\vartheta + \frac{35}{4}\sin\vartheta\cos^2\vartheta\right)e^{i\varphi}, \tag{A.10}
$$

$$
\left(S_{13}^{212,-2} + S_{31}^{212,-2}\right) = -\frac{1}{7\pi}\frac{35}{4}\sqrt{\frac{3}{2}}\sin^3\vartheta\cos\vartheta e^{-3i\varphi}, \tag{A.11}
$$

$$
\left(S_{13}^{2220} + S_{31}^{2220}\right) = \frac{1}{7\pi}\left(\frac{21}{8}\sin^2\vartheta - \frac{105}{8}\sin^2\vartheta\cos^2\vartheta\right)e^{-2i\varphi}, \tag{A.12}
$$

$$
\left(S_{13}^{2221} + S_{31}^{2221}\right) = \frac{1}{7\pi}\sqrt{\frac{35}{2}}\left(-\frac{9}{4}\sin\vartheta\cos\vartheta + \frac{35}{4}\sin\vartheta\cos^2\vartheta\right)e^{-i\varphi}, \tag{A.13}
$$

$$\left(S_{13}^{222,-1}+S_{31}^{222,-1}\right)=\frac{1}{7\pi}\frac{35}{4}\sqrt{\frac{3}{2}}\sin^3\vartheta\cos\vartheta e^{-3i\varphi}, \tag{A.14}$$

$$\left(S_{13}^{2222}+S_{31}^{2222}\right)=-\frac{1}{7\pi}\sqrt{\frac{3}{2}}\left(\frac{7}{8}+\frac{21}{4}\cos^2\vartheta-\frac{35}{8}\cos^4\vartheta\right), \tag{A.15}$$

$$\left(S_{13}^{222,-2}+S_{31}^{222,-2}\right)=-\frac{1}{7\pi}\frac{35}{8}\sqrt{\frac{3}{2}}\sin^4\vartheta\cos\vartheta e^{-4i\varphi}. \tag{A.16}$$

The combinations entering Eqs. (18) for r_M are

$$\begin{aligned} S_{00}(\vartheta,\varphi) &= \operatorname{Re}S_{13}^{2020}+\operatorname{Re}S_{31}^{2020} \\ &= \sqrt{\frac{3}{2}}\left(-\frac{105}{4}\cos^4\vartheta+21\cos^2\vartheta-\frac{7}{4}\right), \end{aligned} \tag{A.17}$$

$$\begin{aligned} S_{01}(\vartheta,\varphi) &= \operatorname{Re}S_{13}^{2021}+\operatorname{Re}S_{31}^{2021}-\operatorname{Re}S_{13}^{202,-1}-\operatorname{Re}S_{31}^{202,-1} \\ &= \left(24\cos\vartheta\sin\vartheta-\frac{105}{2}\sin\vartheta\cos^3\vartheta\right)\cos\varphi, \end{aligned} \tag{A.18}$$

$$\begin{aligned} S_{02}(\vartheta,\varphi) &= \operatorname{Re}S_{13}^{2022}+\operatorname{Re}S_{31}^{2022}+\operatorname{Re}S_{13}^{202,-2}+\operatorname{Re}S_{31}^{202,-2} \\ &= \left(\frac{21}{4}\sin^2\vartheta-\frac{105}{2}\sin^2\vartheta\cos^2\vartheta\right)\cos 2\varphi, \end{aligned} \tag{A.19}$$

$$\begin{aligned} S_{10}(\vartheta,\varphi) &= \operatorname{Re}S_{13}^{2120}+\operatorname{Re}S_{31}^{2120} \\ &= \left(12\cos\vartheta\sin\vartheta-\frac{105}{4}\sin\vartheta\cos^3\vartheta\right)\cos\varphi, \end{aligned} \tag{A.20}$$

$$\begin{aligned} S_{11}(\vartheta,\varphi) &= \operatorname{Re}S_{13}^{2121}+\operatorname{Re}S_{31}^{2121}-\operatorname{Re}S_{13}^{212,-1}-\operatorname{Re}S_{31}^{212,-1} \\ &= \sqrt{\frac{3}{2}}\left(\frac{35}{2}\cos^4\vartheta-\frac{63}{4}\cos^2\vartheta+\frac{7}{4}\right) \\ &\quad+\sqrt{\frac{3}{2}}\left(\frac{35}{2}\cos^4\vartheta-\frac{77}{4}\cos^2\vartheta+\frac{7}{4}\right)\cos 2\varphi, \end{aligned} \tag{A.21}$$

$$\begin{aligned} S_{12}(\vartheta,\varphi) &= \operatorname{Re}S_{13}^{2122}+\operatorname{Re}S_{31}^{2122}+\operatorname{Re}S_{13}^{212,-2}+\operatorname{Re}S_{31}^{212,-2} \\ &= \sqrt{\frac{3}{2}}\left(-\frac{9}{4}\sin\vartheta\cos\vartheta+\frac{35}{4}\sin\vartheta\cos^3\vartheta\right)\cos\varphi \\ &\quad-\frac{35}{4}\sqrt{\frac{3}{2}}\cos\vartheta\sin^3\vartheta\cos 3\varphi, \end{aligned} \tag{A.22}$$

$$\begin{aligned} S_{20}(\vartheta,\varphi) &= \operatorname{Re}S_{13}^{2220}+\operatorname{Re}S_{31}^{2220} \\ &= \left(\frac{21}{8}\sin^2\vartheta-\frac{105}{8}\sin^2\vartheta\cos^2\vartheta\right)\cos 2\varphi, \end{aligned} \tag{A.23}$$

$$
\begin{aligned}
S_{21}(\vartheta,\varphi) &= \operatorname{Re} S_{13}^{2221} + \operatorname{Re} S_{31}^{2221} - \operatorname{Re} S_{13}^{222,-1} - \operatorname{Re} S_{31}^{222,-1} \\
&= \sqrt{\frac{3}{2}}\left(-\frac{9}{4}\sin\vartheta\cos\vartheta + \frac{35}{4}\sin\vartheta\cos^2\vartheta\right)\cos\varphi \\
&\quad - \frac{35}{4}\sqrt{\frac{3}{2}}\sin^3\vartheta\cos\vartheta\cos 3\varphi, \qquad \text{(A.24)}
\end{aligned}
$$

$$
\begin{aligned}
S_{22}(\vartheta,\varphi) &= \operatorname{Re} S_{13}^{2222} + \operatorname{Re} S_{31}^{2222} + \operatorname{Re} S_{13}^{222,-2} + \operatorname{Re} S_{31}^{222,-2} \\
&= -\sqrt{\frac{3}{2}}\left(\frac{35}{8}\cos^4\vartheta - \frac{21}{4}\cos^2\vartheta + \frac{7}{8}\right) - \frac{35}{8}\sqrt{\frac{3}{2}}\sin^4\vartheta\cos 4\varphi. \qquad \text{(A.25)}
\end{aligned}
$$

Further calculations are conveniently carried out in terms of the harmonic variables $x = \sin\vartheta\cos\varphi$, $y = \sin\vartheta\sin\varphi$, and $z = \cos\vartheta$, which satisfy $x^2 + y^2 + z^2 = 1$. One has

$$
\begin{aligned}
&\sin^2\vartheta\cos 2\varphi = 2x^2 + z^2 - 1, \qquad \sin^2\vartheta\cos^2\vartheta\cos 2\varphi = 2x^2z^2 + z^4 - z^2, \\
&\sin^4\vartheta\cos 4\varphi = 8x^4 - 8x^2 + 8x^2z^2 + 1 - 2z^2 + z^4, \\
&\sin\vartheta\cos^3\vartheta\cos\varphi = xz^3, \\
&\cos\vartheta\sin^3\vartheta\cos 3\varphi = 4zx^3 - zx + 3z^3x, \qquad \sin\vartheta\cos\vartheta\cos\varphi = xz. \qquad \text{(A.26)}
\end{aligned}
$$

Accounting for these relations, one finds

$$
\begin{aligned}
S_{00}(x,z) &= \frac{7}{4}\sqrt{\frac{3}{2}}\left(-15z^4 + 12z^2 - 1\right), \qquad S_{01}(x,z) = \frac{3}{2}\left(16xz - 35xz^3\right), \\
S_{02}(x,z) &= \frac{21}{4}\left(2x^2 + 6z^2 - 10x^2z^2 - 5z^4 - 1\right), \\
S_{10}(x,z) &= \frac{1}{4}\left(48xz - 105xz^3\right), \qquad S_{11} = \frac{7}{2}\sqrt{\frac{3}{2}}\left(z^2 + x^2 - 10x^2z^2\right), \\
S_{12}(x,z) &= \frac{1}{2}\sqrt{\frac{3}{2}}\left(48xz - 35xz^3 - 70x^3z\right), \\
S_{20}(x,z) &= \frac{21}{8}\left(2x^2 + 6z^2 - 10x^2z^2 - 5z^4 - 1\right), \\
S_{21}(x,z) &= \frac{1}{2}\sqrt{\frac{3}{2}}\left(48xz - 35xz^3 - 70x^3z\right), \\
S_{22}(x,z) &= -\frac{7}{4}\sqrt{\frac{3}{2}}\left(5z^4 - 8z^2 + 20x^4 - 20x^2 + 20x^2z^2 + 3\right). \qquad \text{(A.27)}
\end{aligned}
$$

We may now evaluate the combinations $R_M(x,z)$ entering Eq. (33):

$$
\begin{aligned}
R_0(x,z) &\equiv \frac{\lambda_2}{\sqrt{6}}S_{02}(x,z) + \frac{\lambda_1}{\sqrt{6}}S_{01}(x,z) + S_{00}(x,z) \\
&= \frac{\sqrt{3}}{4\sqrt{2}}\Big\{7\big[2\lambda_2x^2 + 6(\lambda_2+2)z^2 - 10\lambda_2x^2z^2 - 5(\lambda_2+3)z^4 - \lambda_2 - 1\big] \\
&\qquad + 2\lambda_1\left(16xz - 35xz^3\right)\Big\}, \qquad \text{(A.28)}
\end{aligned}
$$

$$R_1(x,z) \equiv \lambda_2 S_{12}(x,z) + \lambda_1 S_{11}(x,z) + \sqrt{6}\, S_{10}(x,z)$$
$$= \frac{\sqrt{3}}{2\sqrt{2}}\Big\{\big[48(\lambda_2+1)xz - 35(\lambda_2+3)xz^3 - 70\lambda_2 x^3 z\big] + 7\lambda_1\big(z^2 + x^2 - 10x^2z^2\big)\Big\}, \tag{A.29}$$

$$R_2(x,z) \equiv \lambda_2 S_{22}(x,z) + \lambda_1 S_{21}(x,z) + \sqrt{6}\, S_{20}(x,z)$$
$$= \frac{\sqrt{3}}{4\sqrt{2}}\Big\{7\big[-20\lambda_2 x^4 + 2(10\lambda_2+3)x^2 - 10(2\lambda_2+3)x^2z^2 + 2(4\lambda_2+9)z^2 - 5(\lambda_2+3)z^4 - 3\lambda_2 - 3\big] + 2\lambda_1\big(48xz - 35xz^3 - 70x^3z\big)\Big\}. \tag{A.30}$$

Substitution of Eqs. (A.27) into Eqs. (A.28)–(A.30) leads to the results

$$R_0(x,z) = \frac{\sqrt{3}}{4\sqrt{2}}\Big\{7\big[2\lambda_2 x^2 + 6(\lambda_2+2)z^2 - 10\lambda_2 x^2z^2 - 5(\lambda_2+3)z^4 - \lambda_2 - 1\big] + 2\lambda_1\big(16xz - 35xz^3\big)\Big\}, \tag{A.31}$$

$$R_1(x,z) = \frac{\sqrt{3}}{2\sqrt{2}}\Big\{\big[48(\lambda_2+1)xz - 35(\lambda_2+3)xz^3 - 70\lambda_2 x^3 z\big] + 7\lambda_1\big(z^2 + x^2 - 10x^2z^2\big)\Big\}, \tag{A.32}$$

$$R_2(x,z) = \frac{\sqrt{3}}{4\sqrt{2}}\Big\{7\big[-20\lambda_2 x^4 + 2(10\lambda_2+3)x^2 - 10(2\lambda_2+3)x^2z^2 + 2(4\lambda_2+9)z^2 - 5(\lambda_2+3)z^4 - 3\lambda_2 - 3\big] + 2\lambda_1\big(48xz - 35xz^3 - 70x^3z\big)\Big\}. \tag{A.33}$$

References

[1] D. Vollhardt, P. Wölfle, The Superfluid Phases of Helium 3, Taylor & Francis, London, 1990.
[2] R.A. Arndt, C.H. Oh, I.I. Strakovsky, R.L. Workman, F. Dohrmann, Phys. Rev. C 56 (1997) 3005.
[3] M. Hoffberg, A.E. Glassgold, R.W. Richardson, M. Ruderman, Phys. Rev. Lett. 24 (1970) 775.
[4] T. Takatsuka, R. Tamagaki, Prog. Theor. Phys. 46 (1971) 114.
[5] T. Takatsuka, Prog. Theor. Phys. 48 (1972) 1517.
[6] L. Amundsen, E. Østgaard, Nucl. Phys. A 442 (1985) 163.
[7] T. Takatsuka, R. Tamagaki, Prog. Theor. Phys. Suppl. 112 (1993) 27.
[8] V.A. Khodel, V.V. Khodel, J.W. Clark, Phys. Rev. Lett. 81 (1998) 3828.
[9] V.V. Khodel, V.A. Khodel, J.W. Clark, Nucl. Phys. A 679 (2001) 827.
[10] R.B. Wiringa, V.G.J. Stoks, R. Schiavilla, Phys. Rev. C 51 (1995) 38.
[11] J.M.C. Chen, J.W. Clark, R.D. Davé, V.A. Khodel, Nucl. Phys. A 555 (1993) 59.
[12] V.A. Khodel, V.V. Khodel, J.W. Clark, Nucl. Phys. A 598 (1996) 390.

[13] V.A. Khodel, Phys. At. Nucl. 64 (2001) 393.
[14] V.A. Khodel, J.W. Clark, M.V. Zverev, Phys. Rev. Lett. 87 (2001) 031103.
[15] A.B. Migdal, Rev. Mod. Phys. 50 (1978) 107.
[16] A. Akmal, V.R. Pandharipande, D.G. Ravenhall, Phys. Rev. C 58 (1998) 1804.
[17] M. Baldo, Ø. Elgarøy, L. Engvik, M. Hjorth-Jensen, H.-J. Schulze, Phys. Rev. C 58 (1998) 1921.
[18] R.W. Richardson, Phys. Rev. D 5 (1972) 1883.
[19] J.A. Sauls, J.W. Serene, Phys. Rev. D 17 (1978) 1524.
[20] G. Barton, M.A. Moore, J. Phys. C: Solid State Phys. 7 (1974) 2989.